

06.07

Microstructure and electrophysical properties of high-temperature $0.36\text{BiScO}_3-0.64\text{PbTiO}_3$ piezoceramics

© P.A. Pankratiev¹, E.P. Smirnova¹, V.N. Klimov², E.G. Guk¹, N.V. Zaitseva¹,
A.V. Sotnikov³, E.E. Mukhin¹

¹ Ioffe Institute,
St. Petersburg, Russia

² Central Research Institute of Structural Materials „Prometey“,
National Research Centre „Kurchatov Institute“,
St. Petersburg, Russia

³ Emperor Alexander I St. Petersburg State Transport University,
St. Petersburg, Russia

E-mail: pavel-pankratiev@yandex.ru

Received March 7, 2025

Revised March 8, 2025

Accepted March 8, 2025

Microstructure and properties of the $0.36\text{BiScO}_3-0.64\text{PbTiO}_3$ (BSPT) ceramics produced by two different synthesis processes were studied. Ceramics with increased piezoeffect anisotropy (piezoelectric constants ratio $d_{33}/|d_{31}| \approx 5$) was prepared. It was shown that modified two-step synthesis reduces the average grain size of ceramics from $8-10\ \mu\text{m}$ to $0.8-1\ \mu\text{m}$. Considerable improvement of piezoelectric properties of the samples produced by a two step synthesis synthesis process ($d_{33} = 525\ \text{pC/N}$) compared with a single-step process ($d_{33} = 375\ \text{pC/N}$) is observed. Ceramics $0.36\text{BiScO}_3-0.64\text{PbTiO}_3$ produced by the modified two-step process is a promising material for high temperature applications due to a high Curie temperature of $T_C = 430\ ^\circ\text{C}$ and improved piezoelectric properties.

Keywords: BSPT, two-step synthesis, grain size, piezoelectric constants, piezoeffect anisotropy.

DOI: 10.61011/PSS.2025.03.60880.46-25

1. Introduction

Piezoelectric ceramic sensors, ultrasonic transducers and actuators are widely used in many applications such as automotive engineering, iron and steel industry, aerospace industry, transport, nondestructive testing of main pipelines, etc. Many applications require devices that are suitable for a wide temperature range, and in some special cases, operation in a vacuum environment with magnetic fields and intense radiation background must be ensured [1]. Ceramics based on a solid solution of lead zirconate titanate (PZT) are the most widely used. Such ceramics has good piezoelectric properties, however, the Curie temperature T_C depending on the composition is usually not higher than $350\ ^\circ\text{C}$, which restricts the upper temperature limit by a magnitude of about $T_C/2 = 175\ ^\circ\text{C}$ [2]. Materials based on bismuth scandate — lead titanate solid solutions lying near the morphotropic phase boundary (MPB) have been of high interest over the past two decades [3]. The Curie temperature of the $0.36\text{BiScO}_3-0.64\text{PbTiO}_3$ (BSPT) reaches $450\ ^\circ\text{C}$, which is $100\ ^\circ\text{C}$ higher than of PZT Piezoceramics. Moreover, BSPT has piezoelectric properties that are close to, and sometimes even better than, PZT [4].

Piezoceramics properties may be improved by modifying any of the production steps beginning from a compositional change to the final sintering process. Two-step synthesis (sintering) is an effective process for making ceramics with

high density and fine-grained microstructure. This method is successfully used for producing all types of ceramics, including piezoelectric ceramics. Polarized piezoelectric ceramics is known to have the point symmetry group 6mm and, consequently, is characterized by a set of 10 independent material constants: five elastic constants $s_{11}, s_{12}, s_{13}, s_{33}, s_{44}$, three piezoelectric constants d_{31}, d_{33}, d_{15} and two dielectric constants $\epsilon_{11}, \epsilon_{33}$ [5]. Achievement of the full set of material constants for piezoelectric ceramics and of temperature dependences up to high temperatures is critical for the developments of piezoelectric devices. The objective of this study is to determine the primary electrophysical parameters and examine some other physical properties of BSPT ceramic solid solutions produced by a standard process [3] and two-step process [6].

2. Experiment

$0.36\text{BiScO}_3-0.64\text{PbTiO}_3$ ceramics was produced by two processes using a composition obtained by calcination at $850\ ^\circ\text{C}$ for 4 h. The first group of samples was synthesized using a traditional single-step ceramic process that implied ceramic disk firing at $1150\ ^\circ\text{C}$ for 2 h. The second group of samples was made through a modified two-step process: 1 min at $1050\ ^\circ\text{C}$, then the temperature was reduced during 2 h together with furnace cooling down to $800\ ^\circ\text{C}$ and then

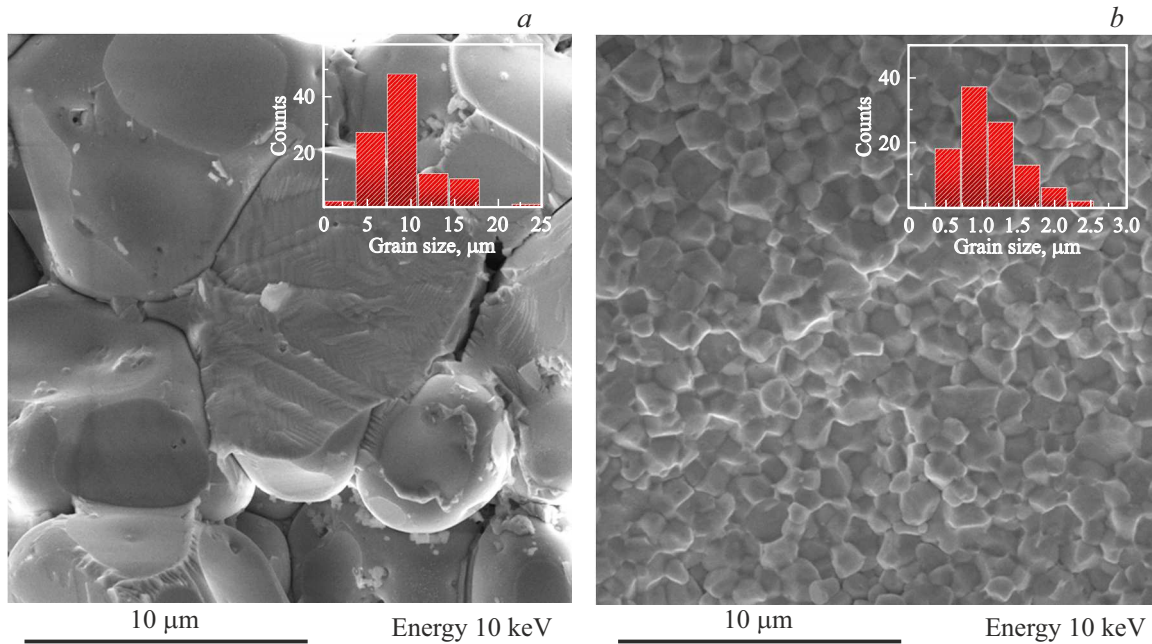


Figure 1. SEM images images of the $0.36\text{BiScO}_3\text{--}0.64\text{PbTiO}_3$ ceramics produced by *a* — a single-step and *b* — two-step processes. The histograms show grain size distribution.

the synthesis was continued for another 4 h. Both synthesis steps, as for the single-step method, were performed in the PbO atmosphere to reduce the loss associated with lead oxide evaporation. Loss of PbO was less than 1%. Silver electrodes were applied by Ag paste firing or by magnetron sputtering. Polarization of the samples was performed at 115°C during 30 min in silicon oil, electric field of $E = 4\text{ kV/mm}$ was applied to the disc thickness. Then particles were cooled down to 40°C in the field for several hours, and then the field was switched off. X-ray diffraction examinations in the 2θ angle range from 10 to 60° were performed using the DRON-3 X-ray diffractometer. Ceramics microstructure was examined using the MIRATESCAN scanning electron microscope (SEM). Piezoelectric constant d_{33} was measured in a static mode by disc thickness variation due to an inverse piezoelectric effect with application of electric fields in the range of $200\text{--}1000\text{ V/mm}$ using the 01IGPC measuring head made by Engineering and Metrology Center „Micro“. Dielectric properties were measured using the R5079 AC bridge (1 kHz, amplitude 1 V), piezoelectric and elastic properties were studied by the resonance–anti-resonance method using the PSM1735 Impedance Analyzer in accordance with IEEE (1987) [7]. Samples for dielectric, piezoelectric and elastic property measurement had a thickness $d = 1\text{ mm}$ and diameter $D = 10\text{ mm}$.

3. Results and discussion

Samples from the first group produced by a single-step process had a smaller density compared with samples

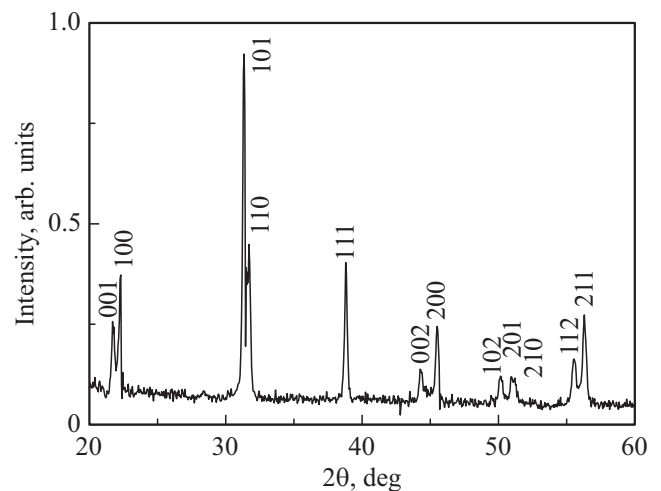


Figure 2. X-ray pattern of the BSPT sample prepared by the single-step synthesis method.

from the second group produced by the modified two-step process (93% vs. 97% of the theoretical value, respectively).

Microstructure of samples differs drastically between the first and second groups. Average ceramics grain size of the second group ($\sim 800\text{ nm}$) is by an order of magnitude less than that of the first group ($\sim 10\ \mu\text{m}$). In addition, grain size distribution histogram of the first ceramics group demonstrates a pronounced peak, while the second ceramics group has a more smeared distribution (Figure 1).

The X-ray diffraction analysis has shown that the samples produced by the modified two-step process (Figure 2)

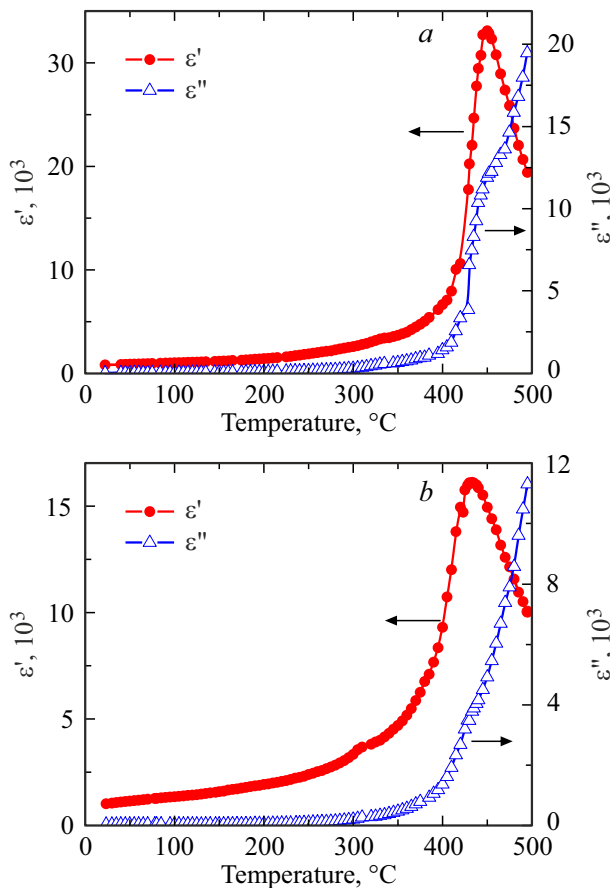


Figure 3. Dependence of the real (ϵ') and imaginary (ϵ'') parts of permittivity on temperature for samples produced by *a* — single-step and *b* — two-step processes.

and single-step process have a similar crystal structure ($P4mm$) located near the morphotropic phase boundary (MPB). However, structural tetragonality of samples made by the two-step synthesis method is $c/a = 1.017$ (where c and a are the lattice cell parameters), which is less than the tetragonality of a compound made by the single-step method ($c/a = 1.025$).

Lattice cell size variations depending on the grain size were addressed in the literature as a sign of deformations induced by internal stresses [8]. In the measured samples, tetragonal distortion characterized by c/a decreases with decreasing grain size. Experimental data may be explained assuming that smaller grain sizes with decreasing tetragonality lead to an increase in mean internal compression stresses in the samples. A comparison is made in the literature between hydrostatic pressure and internal stress effect during grain size reduction due to a difference in the degree of variation of lattice constants a and c . Quantitative pattern of stress distribution in the grain is proposed in [9]. Within this model, stresses are different for grain volume and boundaries, and the vector sum of all stresses across the sample remains equal to zero. It follows from the thermodynamic analysis that the stress will be displayed

as the variation of „spontaneous“ strain, i.e. c/a will decrease [10]. In [11], it is shown that c/a in fine-grained ceramics is lower than in powder made by grinding the same ceramics to a particle size comparable with the grain size. The published data set confirms the assumption that the grain size affects the lattice parameters and occurrence of related internal stresses.

It was also noted that the average grain size affected the ferroelectric phase transition temperature and properties such as permittivity and dielectric loss [12]. Dielectric property measurement showed that the BSPT ceramics synthesis method considerably affected the Curie temperature that was 450°C and 433°C for the single-step and two-step synthesis processes, respectively. Maximum real part of permittivity ϵ' at T_C of the samples produced by the two-step process ($\epsilon'_m = 16000$) is almost twice as low as that of the samples produced by the standard single-step process ($\epsilon'_m = 33000$) (Figure 3). Imaginary parts ϵ'' also differ considerably at T_C : $\epsilon''_{T_C} = 12000$ and $\epsilon''_{T_C} = 3860$ for samples produced by the single-step and two-step synthesis processes, respectively. Similar dependences of the maximum permittivity on the grain size were obtained, for example, for lanthanum-doped lead titanate ceramics [12]. The authors suppose that, as noted above, smaller grain sizes cause an increase in the mean internal compression stresses in the samples and make a comparison between the effect of internal stresses and of hydrostatic pressure on dielectric properties. Therefore, comparison of our data with some published findings regarding the hydrostatic pressure effect on dielectric properties is justified. Thus, Samara [13,14] reported a decrease in maximum dielectric permittivity and an increase in the difference between the temperatures of maximum permittivity and dielectric loss tangent with increasing external hydrostatic pressure for ceramic samples BaTiO_3 .

The piezoelectric resonance–anti-resonance method was used to get also the main electromechanical parameters at room temperature $T = 23^\circ\text{C}$ for two groups of samples, i.e. the planar electromechanical coupling coefficient k_p , piezoelectric constant d_{31} , mechanical Q factor Q_m at the fundamental radial oscillation mode, elastic compliances s_{11} and s_{33} , permittivity ϵ_{33} and dielectric loss tangent $\text{tg}(\delta)$ (see the Table).

Figure 4 shows normalized dependences of the real part of admittance Y' of the samples near the fundamental radial mode frequency. Transition from the single-step to two-step synthesis process shows a considerable increase in FWHM near the resonance frequency, which is indicative of a decrease in Q_m that is defined as a ratio of the resonance frequency to FWHM of the real part of admittance near the resonance frequency [15].

The effect of ceramic grain size on ceramics properties such as ferroelectric phase transition temperature, crystal structure, domain size and, sometimes, density is addressed in a number of papers [16–19]. Note that the findings obtained in this work demonstrate the increase in permittivity and piezoelectric constant in a deep ferroelectric phase at

Measured parameters of the BSPT ceramics made by means of the single-step process (Group 1) and two-step process (Group 2)

Group of samples	$\text{tg}(\delta)$, 1 kHz	ϵ_{33} , 1 kHz	s_{11}^E , $10^{-12} \text{ m}^2/\text{N}$	s_{33}^E , $10^{-12} \text{ m}^2/\text{N}$	d_{33} , pC/N	$-d_{31}$, pC/N	k_p	Q_m
Group 1	0.032	905	17.35	13	350	70	0.34	55
Group 2	0.028	1379	17.08	8.6	525	111	0.48	25

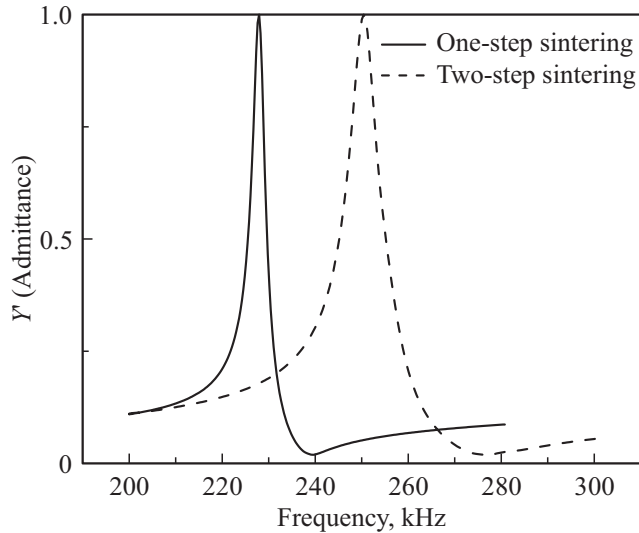


Figure 4. Normalized frequency dependence of the real part of admittance Y' for the fundamental radial oscillation mode of discs produced by the single-step (solid curve) and two-step (dashed curve) processes.

room temperature far away from the ferroelectric transition (see the Table), which is explained within the addressed concepts of the problem. Thus, a considerable increase in permittivity in fine-grained ceramics was observed in BaTiO₃ and attributed to the increase in internal stresses below the Curie point, in particular, due to an increase in [20] and disappearance of [10,20] domain twinning. It was also shown that a decrease in the grain size leads to a decrease in the domain width 90° for elastic field energy and domain wall energy balancing [21]. This situation in turn leads to a decrease in the domain wall sizes. Domain walls with a small area are more active, rotate easily and respond more actively to an external electric field or external physical impact, which facilitates an increase in dielectric and piezoelectric properties [17,21,22]. It is also known that the mechanical Q factor depends strongly on the presence of mobile domain walls, therefore the observed decrease in Q_m with decreasing average grain size may be indicative of the increase in domain wall mobility [23]. It was shown for PZT ceramics that significant amounts of domain walls appear with ceramic grain sizes beginning approximately from 1 μm (lower boundary) [24]. Since the mean grain sizes in both groups of the studied ceramics are $\geq 0.8 \mu\text{m}$, a significant effect of the 90° domain walls on dielectric and

piezoelectric properties in the studied BSPT samples may be expected.

The measurements showed a significant piezoeffect anisotropy in the BSPT ceramics. Thus, $d_{33}/|d_{31}|$ is close to 5 for both groups of samples. High anisotropy of ceramics promotes its suitability for ultrasonic transducers because they generally use only one oscillation mode defined, depending on the type of transducer, by d_{33} or d_{31} , while the other modes induce spurious oscillations and degrade the instrument's performance. Causes of anisotropy occurrence are discussed in theoretical studies as well as on the basis of experimental data. Thus, the calculations showed that piezoelectric constant anisotropy in the PbTiO₃ piezoceramics may depend on other properties, including permittivity anisotropy, and on the mobile 90° domain structure [25]. The effect of high tetragonality [26] and microstructural features such as microcracks and grain sizes [26–28], and of polarizing field and degree of polarization [29] is also addressed. It follows from the theoretical consideration that a very high, including infinite, piezoeffect anisotropy can be actually achieved for piezoceramics because d_{31} can approach zero [30]. It is known that samples made of the modified PbTiO₃ ceramics demonstrate the maximum anisotropy d_{33}/d_{31} equal to 10 [31,32]. Work [28] discusses the growth of piezoelectric constant anisotropy in PZT ceramics when moving away from the morphotropic phase boundary towards increasing content of PbTiO₃ in solid solution, which may also indicate that exactly lead titanate has a high impact on piezoelectric property anisotropy. Thus, the high piezoelectric constant anisotropy detected in the studied BSPT samples might result from a high content of PbTiO₃ and composition localization near MPB on the tetragonal phase side, which is confirmed by the X-ray diffraction analysis [33].

4. Conclusion

Two-step sintering of the 0.36BiScO₃–0.64PbTiO₃ solid solution for ceramic production was used to prepare samples with an average grain size of 800 nm, which is by an order of magnitude smaller than the average grain size (10 μm) of ceramics with the same composition synthesized using the traditional single-step technique. The obtained ceramics features high piezoelectric constant $d_{33} = 525 \text{ pC/N}$ not only compared with the samples produced by the standard process, but also with piezoelectric constants for the known bismuth scandate — lead titanate composition options. The result may be attributed to a set of factors

associated with the effect of internal stresses, including domain size reduction with decreasing grain sizes and appropriately increasing number of mobile domain walls.

Due to a set of properties of ceramics synthesized using the two-step process, i.e. high piezoeffect anisotropy $d_{33}/|d_{31}| \approx 5$, high piezoelectric constants $d_{33} = 525$ pC/N and high Curie temperature ($T_C = 433$ °C), this ceramics is promising for high-temperature piezoelectric transducers and electromechanical actuator applications.

Funding

The study represents a contribution made by the Russian Federation to the ITER project (Rosatom contract No. H.4a.241.19.25) and was supported by the Ministry of Science and Higher Education of the Russian Federation within state assignment 124031800036-2 (FFUG-2024-0034).

Conflict of interest

The authors declare no conflict of interest.

References

- [1] C. Vorpahl, A. Alekseev, S. Arshad, T. Hatae, A. Khodak, J. Klabacha, F. Le Guern, E. Mukhin, S. Pak, C. Seon, M. Smith, E. Yatsuka, A. Zvonkov. *Fusion Eng. Des.* **123**, 11, 712 (2017).
- [2] S. Chen, X. Dong, C. Mao, F. Cao. *J. Am. Ceram. Soc.* **89**, 10, 3270 (2006).
- [3] R.E. Eitel, C.A. Randall, T.R. Shrout, S.-E. Park. *Jpn. J. Appl. Phys.* **41**, 4R, 2099 (2002).
- [4] E.E. Mukhin, V.M. Nelyubov, V.A. Yukish, E.P. Smirnova, V.A. Solovei, N.K. Kalinina, V.G. Nagaitsev, M.F. Valishin, A.R. Belozerova, S.A. Enin, A.A. Borisov, N.A. Deryabina, V.I. Khripunov, D.V. Portnov, N.A. Babinov, D.V. Dokhtarenko, I.A. Khodunov, V.N. Klimov, A.G. Razdobarin, S.E. Alexandrov, D.I. Elets, A.N. Bazhenov, I.M. Bukreev, An.P. Chernakov, A.M. Dmitriev, Y.G. Ibragimova, A.N. Koval, G.S. Kurskiev, A.E. Litvinov, K.O. Nikolaenko, D.S. Samsonov, V.A. Senichenkov, R.S. Smirnov, S.Yu. Tolstyakov, I.B. Tereschenko, L.A. Varshavchik, N.S. Zhiltsov, A.N. Mokeev, P.V. Chernakov, P. Andrew, M. Kempenaars. *Fusion Eng. Des.* **176**, 9, 113017 (2022).
- [5] V.V. Ganopolsky, B.A. Kasatkin, F.F. Legusha, N.I. Prudko, S.I. Pugachev. *Piezokeramicheskie preobrazovateli. Spravochnik. Mashinostroenie, L.* (1984). 256 s. (in Russian).
- [6] T. Zou, X. Wang, W. Zhao, L. Li. *J. Am. Ceram. Soc.* **91**, 1, 121 (2008).
- [7] IEEE Standard on piezoelectricity. ANSI/IEEE Std 176-1987. Institute of Electrical and Electronics Engineers Inc., New York (1987).
- [8] J.L. Jones, E. Aksel, G. Tutuncu, T.-M. Usher, J. Chen, X. Xing, A.J. Studer. *Phys. Rev. B* **86**, 2, 024104 (2012).
- [9] W.W. Kriegel, H. Palmour III. *Mechanical Properties of Engineering Ceramics*. Interscience, New York (1961). 646 s.
- [10] W.R. Buessem, L.E. Cross, A.K. Goswami. *J. Am. Ceram. Soc.* **49**, 1, 33 (1966).
- [11] G.H. Jonker, W. Noorlander. In: *Science of ceramics, v. I / Ed. G.H. Stewart*. Academic Press, London (1962). P. 255.
- [12] K. Keizer, A.J. Burggraaf. *Physi Status Solidi A* **26**, 2, 561 (1974).
- [13] G.A. Samara. *Phys. Rev.* **151**, 2, 378 (1966).
- [14] G.A. Samara. *Ferroelectrics* **2**, 1, 277 (1971).
- [15] V/L/zemlyakov. *Metody i sredstva izmerenij v piezoelektricheskom priborostroenii*. Izd-vo YuFU, Rostov-na-Donu (2009) 179 s. (in Russian).
- [16] Y. Dong, Z. Zhou, R. Liang, X. Dong. *J. Am. Ceram. Soc.* **103**, 9, 4785 (2020).
- [17] H. Ghayour, M. Abdellahi. *Powder Technol.* **292**, 84 (2016).
- [18] Y. Huan, X. Wang, J. Fang, L. Li. *J. Am. Ceram. Soc.* **96**, 11, 3369 (2013).
- [19] Y. Huan, X. Wang, J. Fang, L. Li. *J. Eur. Ceram. Soc.* **34**, 5, 1445 (2014).
- [20] G. Arlt. *J. Mater. Sci.* **25**, 6, 2655 (1990).
- [21] G. Arlt, D. Hennings, G. de With. *J. Appl. Phys.* **58**, 4, 1619 (1985).
- [22] N. Ma, B.-P. Zhang, W.-G. Yang, D. Guo. *J. Eur. Ceram. Soc.* **32**, 5, 1059 (2012).
- [23] B. Jaffe, W.R. Cook, H. Jaffe. *Piezoelectric ceramics*. Academic Press, London (1971). 302 p.
- [24] B.A. Tuttle, T.J. Garino, J.A. Voigt, T.J. Headly, D. Dimos, M.O. Eatough. In: *Science and Technology of Electroceramic Thin films / Eds O. Auciello, R. Waser*. Kluwer Academic Publishers, Dordrecht (1995). P. 177.
- [25] A.V. Turik, V.Yu. Topolov. *J. Phys. D: Appl. Phys.* **30**, 11, 1541 (1997).
- [26] A.N. Rybyanets, M.A. Lugovaya, G.M. Konstantinov, N.A. Shvetsova, D.I. Makarev. *Bull. RAS: Phys.* **82**, 3, 246 (2018).
- [27] A.J. Danziger, O.N. Razumovskaya, L.A. Reznichenko, V.P. Sakhnenko, A.N. Klevtsov, S.I. Dudkina, L.A. Shilkina, N.V. Dergunova, A.N. Rybyanets. *Mnogokomponentnye sistemy segnetoelektricheskikh slozhnykh oksidov: fizika, kristallohimiya, tekhnologiya. Aspekty dizajna p'ezoelektricheskikh materialov. Izd-vo YuFU, Rostov-na-Donu (2001)*. V. 1, 408 s., t. 2, 365 s. (in Russian).
- [28] W. Wersing, K. Lubitz, J. Mohaupt. *IEEE Trans. Ultrason. Ferroelectr. Freq. Control* **36**, 4, 424 (1989).
- [29] A.G. Luchaninov, L.A. Shuvalov. *Crystallogr. Reps* **44**, 2, 263 (1999).
- [30] V.Yu. Topolov, E.I. Bondarenko, A.V. Turik, A.I. Chernobobov. *Ferroelectrics* **140**, 1, 175 (1993).
- [31] H. Watanabe, K. Nakamura, H. Shimizu. *IEEE Trans. Sonics & Ultrason.* **28**, 4, 265 (1981).
- [32] V.Yu. Topolov, A.E. Panich. *Elektronny zhurnal „Issledovano v Rossii“* **11**, 8 (2008). <http://zhurnal.apec.reln.ru/articles/2008/002.pdf>
- [33] E.G. Guk, E.P. Smirnova, V.N. Klimov, P.A. Pankratiev, N.V. Zaitseva, A.V. Sotnikov, E.E. Mukhin. *FTT* **66**, 8, 1397 (2024). (in Russian).

Translated by E.Ilnskaya